On the behavior of velocity gradient tensor invariants in direct numerical simulations of turbulence

Brian J. Cantwell
Department of Aeronautics and Astronautics, Stanford University, Stanford, California 94305

(Received 4 January 1993; accepted 7 April 1993)

Studies of direct numerical simulations of incompressible, homogeneous, and inhomogeneous turbulence indicate that, in regions of high kinetic energy dissipation rate, the geometry of the local velocity gradient field has a universal character. The velocity gradient tensor satisfies the nonlinear evolution equation $(dA_{ij}/dt)+A_{ik}A_{kj}-1/3(A_{mn}A_{nm})\delta_{ij}=H_{ij}$ where $A_{ij}=\partial u_i/\partial x_j$ and the tensor H_{ij} contains terms involving the action of cross derivatives of the pressure field and viscous diffusion of A_{ij}. The restricted Euler equation corresponding to $H_{ij}=0$ can be solved in closed form [Cantwell, Phys. Fluids A **4**, 782 (1992)] and the solution has the property that, for any initial condition, $A_{ij}(t)$ evolves to an asymptotic state of the form $A_{ij}(t)\cong K_{ij}[R(t)]^{1/3}$ where $R(t)$ is a function which becomes singular in a finite time and K_{ij} is a constant matrix. A number of the universal features of fine-scale motions observed in direct numerical simulations are reproduced by K_{ij}. In the simulation studies the first invariant of A_{ij} is zero by incompressibility. The second and third invariants, Q and R, are determined at every grid point in the flow and the entire data set is cross-plotted to search for significant features in the space of tensor invariants. Such features can then be associated with corresponding local flow structures in physical space. When a variety of incompressible simulations are studied, scatter plots of Q vs R reveal that a fairly significant fraction of the data lies in the lower right quadrant. This is consistent with behavior predicted by the restricted Euler solution. However, the bulk of the data lies more or less uniformly distributed in a slightly elliptical region about the origin. In a direct numerical simulation of a plane, time-developing, mixing layer a small fraction of the data collects along a very pronounced, nearly straight, ridgeline extending into the upper left quadrant. This data can be traced to regions with local vorticity much larger than the local strain lying within streamwise rib vortices which connect adjacent spanwise rollers in the mixing layer simulation. Neither the predominant tendency for Q and R to lie near the origin nor the possibility for Q and R to lie far from the origin in the upper left quadrant are predicted by the restricted Euler solution. The purpose of this paper is to show that, by relaxing the assumption $H_{ij}=0$ while retaining a model of dA_{ij}/dt motivated by the asymptotic form of the restricted Euler solution, one can begin to account for these features of the (Q,R) scatter plots. The results suggest that the velocity gradient tensor in three-dimensional flow tends to evolve toward an attractor in the space of tensor invariants. A significant feature of the model is that, although $H_{ij}\neq 0$, singular behavior of $A_{ij}(t)$ can still occur along specific paths in the (Q,R) plane corresponding to zero values of the discriminant of H_{ij}.

I. THE RESTRICTED EULER SOLUTION FOR $H_{ij}=0$

The incompressible Navier–Stokes equations

$$\frac{du_i}{dt}=-\frac{\partial p}{\partial x_i}+\nu\frac{\partial^2 u_i}{\partial x_k\,\partial x_k} \tag{1}$$

are differentiated with respect to x_j and the Poisson equation for the pressure is subtracted from both sides leading to the transport equation for the velocity gradient tensor

$$\frac{dA_{ij}}{dt}+A_{ik}A_{kj}-\frac{1}{3}(A_{mn}A_{nm})\delta_{ij}=H_{ij}, \tag{2}$$

where $A_{ij}=\partial u_i/\partial x_j$, the tensor H_{ij} is given by

$$H_{ij}=-\left(\frac{\partial^2 p}{\partial x_i\,\partial x_j}-\frac{\partial^2 p}{\partial x_k\,\partial x_k}\frac{\delta_{ij}}{3}\right)+\nu\frac{\partial^2 A_{ij}}{\partial x_k\,\partial x_k} \tag{3}$$

and p is the kinematic pressure (pressure/density). Equation (2) is used to generate equations for the invariants $Q(t)$ and $R(t)$,

$$\frac{dQ}{dt}+3R=-A_{mn}H_{nm},\quad \frac{dR}{dt}-\frac{2}{3}Q^2=-A_{mn}A_{nk}H_{km}, \tag{4}$$

where

$$Q=-\tfrac{1}{2}A_{mn}A_{nm},\quad R=-\tfrac{1}{3}A_{mn}A_{nk}A_{km}. \tag{5}$$

The first invariant $P=-A_{ii}=0$ by incompressibility. Differentiating (2) with respect to time leads to

$$\frac{d^2A_{ij}}{dt^2}+\frac{2}{3}Q(t)A_{ij}=\frac{dH_{ij}}{dt}-A_{ik}H_{kj}-H_{ik}A_{kj}+\frac{2}{3}(A_{mn}A_{nm})\delta_{ij}. \tag{6}$$

The restricted Euler system corresponding to the homogeneous case, $H_{ij}=0$, $dH_{ij}/dt=0$, has been solved in closed form for $A_{ij}(t)$.[1] The main properties of the solution

 0899-8213/93/5(8)/2008/6/$6.00

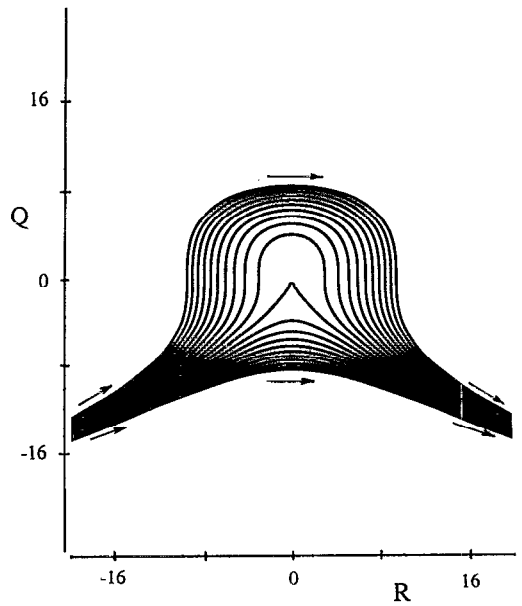

FIG. 1. Family of solutions of the restricted Euler system. Arrows indicate direction of increasing time.

are that $A_{ij}(t)$ becomes singular in a finite time and $Q(t)$ and $R(t)$ evolve along lines of constant discriminant, D, where

$$D=Q^3+\tfrac{27}{4}R^2=Q_i^3+\tfrac{27}{4}R_i^2=Q_0^3. \tag{7}$$

The family of solutions (7) is shown in Fig. 1. The quantities Q_i and R_i are the initial values of the invariants and Q_0 defines a time scale for the evolution of $A_{ij}(t)$

$$t_0=1/\sqrt{\text{abs}(Q_0)}. \tag{8}$$

In the case where $Q_0=0$, the characteristic time is $t_0=1/\sqrt{-Q_i}$ and the invariants evolve along the lines $R=\pm(-\frac{4}{27}Q^3)^{1/2}$ which separate real and complex eigenvalues of A_{ij}. The quantities $Q(t)$ and $R(t)$ are expressed in terms of Jacobian elliptic functions and, as with the individual components of A_{ij}, they become singular in a finite time except for a set of initial conditions of zero measure corresponding to $Q_0=0$, $R_i<0$. In the latter case Q and R evolve to zero while the individual components of A_{ij} become singular. The evolution to singularity is very rapid occurring in just a few characteristic times. Vieillefosse[2] has described this situation physically as the free motion of a fluid element which rotates and deforms under its own strain and vorticity field while conserving angular momentum about its center of mass.

For any initial condition other than $Q_0=0$, $R_i<0$, the restricted Euler solution evolves to the asymptotic form

$$A_{ij}(t)\cong K_{ij}[R(t)]^{1/3}, \tag{9}$$

where the matrix defining the asymptotic state, K_{ij}, satisfies the algebraic equation

$$K_{ij}+2^{1/3}K_{ik}K_{kj}-2^{2/3}\delta_{ij}=0. \tag{10}$$

The invariants of K_{ij} are $(P_K,Q_K,R_K)=(0,-3/2^{2/3},1)$, and lie on the line $R_K=(-\frac{4}{27}Q_K^3)^{1/2}$. Thus according to the restricted Euler solution the invariants Q and R evolve to the lower right quadrant as indicated by the arrows in Fig. 1. The matrix K_{ij} can be decomposed into a symmetric and an antisymmetric part $K_{ij}=S_{ij}+W_{ij}$ and upon examination it is found that solutions of (10) have the following properties:

(i) Two of the principal rates of strain are positive, one is negative.

(ii) The vorticity vector is aligned exactly with the smaller positive principal rate of strain.

For purposes of the later discussion it should be pointed out here that if the sign of the leftmost term in (10) is made negative the geometry (i) and (ii) is reversed, i.e., two of the principal rates of strain are negative and the vorticity is aligned with the intermediate negative rate of strain. The positivity of the leftmost term in (10) reflects the fact that, in the restricted Euler solution, dA_{ij}/dt is positive as the solution approaches the asymptotic state. This is consistent with the analysis of Betchov[3] who showed that in isotropic turbulence $\partial\langle\omega_i\omega_i\rangle/\partial t=-\langle abc\rangle+$viscous terms where $\langle\omega_i\omega_i\rangle$ is the mean square vorticity and $\langle abc\rangle$ is the mean of the product of principal rates of strain a, b, and c. The tendency for the intermediate rate of strain to be positive or negative depends on whether the enstrophy is increasing or decreasing with time. In all of the simulations studied to date,[4–7] in regions of high kinetic energy dissipation, the velocity gradient tensor has the properties (i) and (ii) with the probability that the vorticity is aligned with the smaller positive rate of strain approaching one as the data is conditioned on higher and higher rates of dissipation.

The restricted Euler model is predicated on the assumption that $H_{ij}=0$ implying that, except for the constraint imposed by continuity, adjacent fluid elements cannot affect one another through the pressure and viscous stress field. It is rather remarkable that such an oversimplified model would have a close correspondence to direct numerical simulations of the full Navier–Stokes equations. The results suggest that the restricted Euler solution plays a role in real flows. It appears that an important element in the dynamics of kinetic energy dissipation is the tendency for fluid elements to evolve toward singularity via the restricted Euler route even though singularity does not actually occur.

The restricted Euler solution has the property that the invariants Q and R always evolve to the lower right quadrant ($Q<0,R>0$) as indicated in Fig. 1. When (Q,R) data from a direct numerical simulation by Moser and Rogers[8] of a plane time-developing mixing layer is plotted the result is something quite different as shown in Fig. 2. The case shown here is designated HIGH/P in the terminology of Moser and Rogers,[8] Table 2. The procedure used to produce this figure is to evaluate Q and R at an instant at every grid point in the numerically computed flow and then produce a scatter plot in the (Q,R) plane. In the actual scatter plot the region near the origin is completely obscured by layers and layers of overlapping points. To remedy this, contours of the logarithm of the number density are plotted instead. The lowest contour level is set at one so that

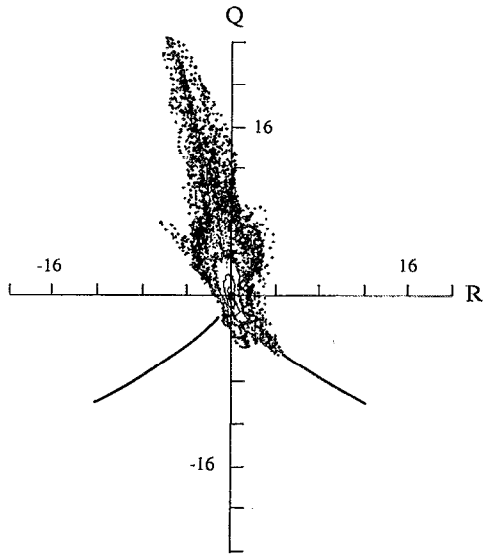

FIG. 2. Number density contour plot of velocity gradient tensor invariants from direct numerical simulation of a plane mixing layer by Moser and Rogers.[8] Dimensionless time $tU_0/\delta=29.8$ where δ is the initial vorticity thickness and U_0 is one-half the velocity difference across the layer. For further details see Ref. 5.

isolated points are captured, this retains the features of the scatter plot far from the origin while providing information about the structure of the Q, R distribution near the origin.

Figure 2 is a snapshot of the current values of the invariants for a large number of particles at various stages of evolution from a range of local initial conditions on the velocity gradient tensor. There are three significant features of Fig. 2 which this paper is intended to address. These are as follows:

(a) A significant fraction of the data lies in the lower right quadrant along the ($R>0$, $D=0$) branch. These points are characterized by relatively high rates of kinetic energy dissipation. This feature of Fig. 2 is consistent with behavior predicted by the restricted Euler solution.

(b) By far the preponderance of points collects in an elliptical region about the origin with its major axis aligned with the upper left and lower right quadrants. The restricted Euler solution does not predict this feature although the presence of a cusp at the origin in Fig. 1 is indicative of a slowing down of the evolution of invariants for particles with Q_0 close to zero (t_0 large). Particles close to the cusp will remain so for a long time.

(c) A small fraction of the data collects along a very pronounced, nearly straight, ridgeline extending into the upper left quadrant. This feature of Fig. 2 is not at all predicted by the restricted Euler solution. The local topology in this region is of the type stable-focus-stretching[9] and, for points far from the origin, the local vorticity strongly dominates the local strain. Moreover, points far from the origin tend to be associated with relatively small rates of kinetic energy dissipation (cf. Ref. 5, Fig. 10).

While only one flow case is presented here, a variety of simulations have been studied[5–7] and in all cases one observes the sort of distribution of points around $(Q,R)=(0,0)$ shown in Fig. 2 [features (a) and (b)]. What is not always observed is the ridge extending into the upper left quadrant [feature (c)]. This seems to be a feature characteristic of the early evolution of an inhomogeneous flow started with laminar initial conditions. In the mixing layer these points can be traced in physical space to relatively long-lived rib vortices which connect adjacent large spanwise rollers and which remain identifiable during the first couple of vortex pairings.[5,10] In simulations of homogeneous shear flow[6] the ridge is not seen.

Neither the predominant tendency for Q and R to lie near the origin nor the possibility for Q and R to lie along a roughly straight ridgeline in the upper left quadrant are permitted by the restricted Euler solution.

II. AN INTERMEDIATE ASYMPTOTIC MODEL FOR $H_{ij}\neq 0$

It is extremely difficult to predict how the velocity gradient tensor should evolve in a general flow. This is due to the fact that it is virtually impossible to make any broad statements about the terms which appear in H_{ij} given in (3). This is particularly true of the pressure field which is the solution of a Poisson equation and thus depends on the entire flow. We expect that viscous diffusion would limit the growth of A_{ij} but other than this very little can be said without considering specific cases and even then the problem of identifying general, local properties of the cross derivatives of the pressure remains a formidible obstacle. The whole question of whether singularities can develop in rotational solutions of the Euler and/or Navier–Stokes equations remains a controversial subject. There have been a number of efforts to identify singular behavior by the direct numerical computation of solutions of the Euler equations with smooth initial conditions.[11,12] Most recently Kerr[13] has computed a flow which appears to exhibit genuinely singular behavior. A significant feature of this computation is that it computes a flow which contains a high degree of symmetry and the maintenance of the symmetry is essential to the continuance of the solution toward singularity. This point will be returned to later.

The purpose of this paper is to show that, by relaxing the assumption $H_{ij}=0$ while retaining a model of dA_{ij}/dt motivated by the asymptotic behavior of the restricted Euler solution (9), one can begin to account for features (b) and (c) of Fig. 2. The basic assumption of the model is the following: That some time after a fluid particle is set into motion by the flow, during which various components of A_{ij} may change at different rates, the particle settles into a state similar to (9) where its angular momentum changes relatively slowly under the action of relatively weak torques arising from $H_{ij}\neq 0$. That is, we hypothesize the existence of an intermediate asymptotic state for $A_{ij}(t)$ during which it behaves as

$$A_{ij}(t)=M_{ij}e^{\int f(t)dt},\quad \frac{dA_{ij}}{dt}=A_{ij}f(t), \tag{11}$$

where M_{ij} is a constant matrix. In the restricted Euler solution $f(t)=\frac{1}{3}[d(\ln R)/dt]$, however, in the present context we will simply regard $f(t)$ as an arbitrary scalar function of time.

The use of the term "intermediate" needs to be clarified. One can argue for the ansatz (11) by recognizing that H_{ij} fluctuates and can change sign. If, in the evolution of a particle, H_{ij} becomes small and remains small for a finite period then there will be a tendency for the local A_{ij} to begin to follow the restricted Euler solution. This solution has the property that the evolution to the asymptotic state (9) is achieved very rapidly and this adds support to the plausibility of the model at least for some subset of fluid particles. In a sense, the restricted Euler solution and its associated tendency to rapidly amplify velocity gradients is always available, ready to drive up the gradients in the neighborhood of a fluid particle when local conditions on H_{ij} permit. Diffusion and/or the anisotropic pressure terms in (3) may cut off the process but perhaps not before the behavior (11) is realized for some period of time. In this sense the behavior (11) is viewed as an intermediate state in the evolution of a fluid particle. The argument for (11) can be made rigorously in the case of one or two parameter flows invariant under $x_i=e^{a}\hat{x}_i$, $t=e^{a/k}\hat{t}$, $u_i=e^{a(k-1)/k}\hat{u}_i$, $p=e^{a(2k-2)/k}\hat{p}$, the stretching transformation group of the Euler (k arbitrary) and Navier–Stokes ($k=1/2$) equations.[14] This class of similarity flows, for which $f(t)=-1/t^2$, is discussed in Ref. 15.

Using (11) Eq. (2) becomes an algebraic relationship between A_{ij} and H_{ij},

$$fA_{ij}+A_{ik}A_{kj}-1/3(A_{mn}A_{nm})\delta_{ij}=H_{ij}. \tag{12}$$

This gives us an opportunity to learn something fairly general about the effect of nonzero H_{ij} on the behavior of A_{ij} albeit within the confines of the assumptions about the intermediate asymptotic state. The procedure involves first squaring and then cubing both sides of (12). The Cayley–Hamilton theorem is used to reduce higher-order products of A_{ij} and then the trace of H^2 and H^3 is formed. The result is

$$Q_H=f^2Q+3fR-\tfrac{1}{3}Q^2 \tag{13}$$

and

$$R_H=f^3R-fQR-\tfrac{2}{3}f^2Q^2-\tfrac{2}{27}Q^3-R^2, \tag{14}$$

where

$$Q_H=-\tfrac{1}{2}H_{mn}H_{nm},\quad R_H=-\tfrac{1}{3}H_{mn}H_{nk}H_{km}. \tag{15}$$

Now a rather interesting thing happens. When we square (14) and cube (13), add the two together and factor the result, we find the following relationship between the discriminants of A_{ij} and H_{ij}:

$$Q_H^3+\tfrac{27}{4}R_H^2=(Q^3+\tfrac{27}{4}R^2)(R+fQ+f^3)^2. \tag{16}$$

Note that terms on the right-hand side of order (Q^6) have canceled. Note further that the second factor on the right-hand side of (16) is squared from which we conclude that, during the intermediate asymptotic state, the discriminants of A_{ij} and H_{ij} have the same sign, i.e., the eigenvalues have the same character. In particular, complex eigenvalues of A_{ij} cannot occur unless the antisymmetric part of the viscous diffusion term in (3) is included in H_{ij}. Referring back to Fig. 2 one might conjecture on this basis that the relatively long life of the rib vortices in the mixing layer computation is attributable to the role of viscosity in helping to prevent the collapse to a flow with real eigenvalues which would otherwise occur if the viscous term were absent.

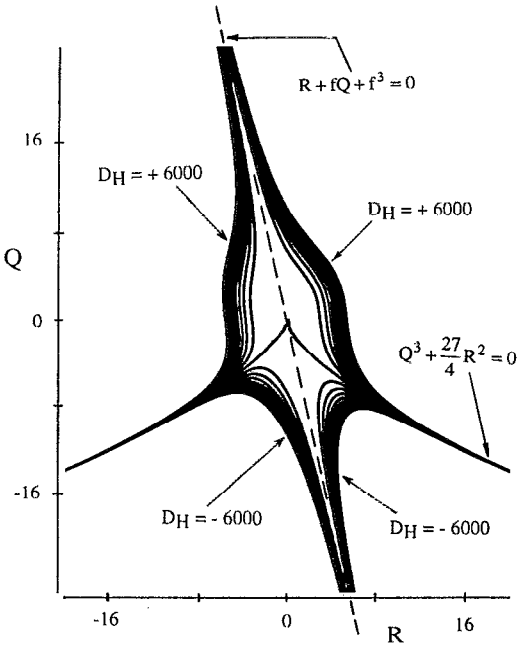

FIG. 3. Contours of constant $D_H=Q_H^3+\frac{27}{4}R_H^2$ with $f(t)=0.22$ [see Eq. (16)].

In the restricted Euler solution discussed earlier the velocity gradient tensor becomes singular in a finite time and the invariants asymptote to $Q=-(\frac{27}{4}R^2)^{1/3}$; $R>0$. Here we see that when H_{ij} is permitted to be nonzero a new structure appears in the space of tensor invariants of A_{ij}. This is shown in Fig. 3 which depicts contours of the right-hand side of (16) where a value of $f(t)=0.22$ has been used to match the slope of the ridgeline in Fig. 2. The zeros of (16) are also indicated on the figure. It is not obvious at the scale of Fig. 3 but there is a point of osculation between the zeros of (16). Thus for $(-\infty<f<\infty)$ the straight line $R+fQ+f^3=0$ is the generator of $Q^3+(\frac{27}{4})R^2=0$. While, in principle, Q and R can range over the whole space, extremely large values of the discriminant $D_H=Q_H^3+\frac{27}{4}R_H^2$ would be required to move away from the very steep-sided, and I think rather beautiful, surface depicted in Fig. 3. Figure 4 shows the minimum ($D_H=-6000$), maximum ($D_H=+6000$) and zero contours of Fig. 3 superimposed on the data from Fig. 2. To reinforce the point just made, if the contours had been chosen to range from, say, $-60\,000$ to $+60\,000$ Figs. 3 and 4 would be relatively little changed. In effect, the surface (16) defines a region of attraction in the space of tensor invariants of A_{ij}. In general, the observations from direct numerical simulation support the conclusion that

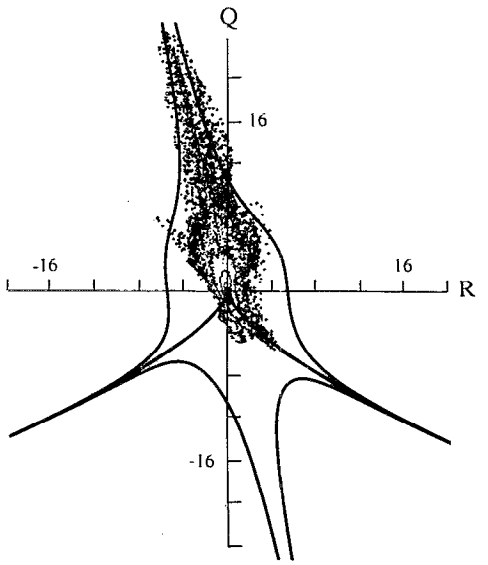

FIG. 4. Data from Fig. 2 superimposed on maximum, minimum, and zero contours of Fig. 3.

very large values of D_H probably do not occur.

In the intermediate asymptotic model with $H_{ij} \neq 0$ singular behavior is no longer a necessary property of the solution as in the restricted Euler case. Indeed Q and R would seem most likely to cluster near (0,0) as is the case in Figs. 2 and 4. *Nevertheless singular behavior is not ruled out and in fact, as is clearly shown in Fig. 3, it is the zeros of (16) that define the possible paths to singularity.* Moreover, at large Q and R the zeros of D_H lie close to large values of D_H. In this respect large D_H is not a necessary condition for singular behavior. It is quite possible to encounter large values of D_H during a computation while simultaneously being very close to $D_H=0$. From the evidence of simulations and the asymptotic behavior of the restricted Euler solution it would appear that the most accessible route to singularity is along the ($D=0$, $R>0$) branch in the (Q,R) plane. In the parlance of Ref. 9 this is a flow catagorized as unstable node–saddle–saddle with real eigenvalues in the ratio (1/2, 1/2, −1). Imposition on an Euler calculation of symmetries sufficient to satisfy the assumption (11) for some subset of particles and careful enforcement of those symmetries so as to permit the particles to evolve locally along the ($D=0$, $R>0$) branch should generate singular behavior and this may help to explain the success of Kerr's[13] approach.

It has been pointed out by Jimenez[16] that, in the neighborhood of a localized region of stretched vorticity, the geometry of the strain and vorticity field near the radius of maximum dissipation will be characterized by (i) and (ii) when the maximum vorticity is much larger than the ambient. The Burgers' vortex is used to illustrate the point although some care is required since, for the Burgers' vortex solution, the ratio of maximum vorticity to ambient is infinite for all Reynolds numbers but the geometry (i) and (ii) only occurs when the Reynolds number of the Burgers' vortex exceeds a threshold value.

While this helps to explain the kinematic conditions under which the geometry (i) and (ii) might occur it does not explain the tendency for a general three-dimensional flow to evolve to such a state. For a two-dimensional flow with out-of-plane straining the velocity gradient tensor is of the form

$$A_{ij}=\begin{bmatrix} A_{11} & A_{12} & 0 \\ A_{21} & A_{22} & 0 \\ 0 & 0 & b \end{bmatrix}, \tag{17}$$

where b is the rate of strain in the third direction. If b is positive, the flow is subjected to out-of-plane stretching (see, for example, the steady Burgers' vortex, the Lundgren spiral,[17,18] etc.). Negative b corresponds to out-of-plane compression for which no steady state generally exists. It can be easily shown that the invariants of (17) satisfy

$$R+bQ+b^3=0, \tag{18}$$

a form we have just encountered in the attractor (16). That (18) arises naturally in (16) through a fairly basic analysis of the equations of motion is significant. The intermediate asymptotic model suggests that local flow structures characterized by (18) should evolve as typical features of turbulent flow. It is surprising that an extended region of the flow (i.e., the rib vortex) should be characterized by a nearly constant value of $f(t)$ as seems to be indicated in Fig. 4. However, it needs to be emphasized that, in terms of vorticity, the rib vortex is the most intense structure in the flow and therefore is the most apparent in the (Q,R) scatter plot. Evidence for weaker structures with different f's can also be seen in Fig. 4 and indeed examination of a variety of flow structures most of which are buried near the origin of the (Q,R) plot would reveal a wide range of mostly positive f's.

III. CONCLUDING REMARKS

In the restricted Euler solution $f(t)$ is a universal function for all particles. The simulation results shown in Fig. 2 indicate that there may be finite-sized regions of the flow where, at a given instant, $f(t)$ may have approximately the same value. However, even if $f(t)$ has universal properties it would not be readily apparent in a plot such as Fig. 2. All the simulations studied to date are initiated from small disturbance initial conditions superimposed on an unstable base flow. As instabilities develop the invariants of the velocity gradient tensor soon acquire a wide range of values. As a result different particles would reach the intermediate asymptotic state at different times and with a wide range of time scales (8). In effect one has to consider $f[(t-t_n)/t_{0n}]$ where n is the index of the nth particle and t_{0n} represents a local time scale [cf. Eq. (8)]. A search for the existence of the intermediate asymptotic state and the properties of $f(t)$ will require a detailed study of the Lagrangian characteristics of simulations which have been computed long enough to reach a fully developed equilibrium state. Nevertheless the basin surrounding the origin $(Q,R)=(0,0)$ is a very robust feature of the attractor (16) and is largely independent of $f(t)$.

The intermediate asymptotic model and the evidence from simulations suggests that the velocity gradient tensor in turbulent flows evolves to an attractor in the space of tensor invariants and that the restricted Euler solution plays a significant role in the dynamics of kinetic energy dissipation. The topography of this attractor, with a basin near the origin traversed by (18) indicates that local flow structures characterized by Q and R close to zero or by out-of-plane straining of a locally two-dimensional flow should evolve as typical features of turbulent flows.

ACKNOWLEDGMENT

This work is supported by Office of Naval Research Grant No. N00014-90-J-1976.

[1]B. J. Cantwell, "Exact solution of a restricted Euler equation for the velocity gradient tensor," Phys. Fluids A **4**, 782 (1992).
[2]P. Vieillefosse, "Internal motion of a small element of fluid in an inviscid flow," Physica A **125**, 150 (1984).
[3]R. Betchov, "An inequality concerning the production of vorticity in isotropic turbulence," J. Fluid Mech. **1**, 497 (1956).
[4]W. T. Ashurst, R. Kerstein, R. Kerr, and C. Gibson, "Alignment of vorticity and scalar gradient with strain rate in simulated Navier–Stokes turbulence," Phys. Fluids **30**, 2343 (1987).
[5]J. H. Chen, M. S. Chong, J. Soria, R. Sondergaard, A. E. Perry, M. Rogers, R. Moser, and B. J. Cantwell, "A Study of the topology of dissipating motions in direct numerical simulations of time-developing compressible and incompressible mixing layers," *Proceedings of the 1990 CTR Summer Program* (Center for Turbulence Research, Stanford, CA, 1990).
[6]R. Sondergaard, J. H. Chen, J. Soria, and B. Cantwell, "Local topology of small scale motions in turbulent shear flows," in the Eighth Symposium on Turbulent Shear Flows, Munich, 9–11 September 1991.
[7]J. Soria, M. S. Chong, R. Sondergaard, A. E. Perry, and B. J. Cantwell, "A study of the fine scale motions of incompressible time-developing mixing layers," *Proceedings of the 1992 CTR Summer Program* (Center for Turbulence Research, Stanford, CA, 1992).
[8]R. Moser and M. Rogers, "The three-dimensional evolution of a plane mixing layer: pairing and transition to turbulence," J. Fluid Mech. **247**, 275 (1993).
[9]M. S. Chong, A. E. Perry, and B. J. Cantwell, "A general classification of three-dimensional flow fields," Phys. Fluids A **2**, 765 (1990).
[10]J. M. Lopez and C. J. Bulbeck, "Behavior of streamwise rib vortices in a three dimensional mixing layer," in Ref. 7.
[11]A. Pumir and E. Siggia, "Collapsing solutions to the 3-D Euler equations," Phys. Fluids A **2**, 220 (1990).
[12]R. M. Kerr and F. Hussain, "Simulation of vortex reconnection," Physica D **37**, 474 (1989).
[13]R. M. Kerr, "Evidence for a singularity of the three-dimensional, incompressible Euler equations," submitted to Phys. Fluids A.
[14]B. J. Cantwell, "Organized motion in turbulent flow," Annu. Rev. Fluid Mech. **13**, 457 (1981).
[15]B. J. Cantwell, "Geometry of turbulent fine scale structure," in *The 11th Australasian Fluid Mechanics Conference,* Hobart, Australia, 14–18 December 1992 (University of Tasmania, Hobart, Australia, 1992).
[16]J. Jimenez, "Kinematic alignment effects in turbulent flows," Phys. Fluids A **4**, 652 (1992).
[17]T. S. Lundgren, "Strained spiral vortex model for turbulent fine structure," Phys. Fluids **25**, 2193 (1982).
[18]D. I. Pullin and P. G. Saffman, "On the Lundgren–Townsend model of turbulent fine scales," Phys. Fluids A **5**, 126 (1993).